# A Versatile Hybrid Agent-Based, Particle and Partial Differential Equations Method to Analyze Vascular Adaptation *

Marc Garbey[1,2,3], Stefano Casarin[1,3], and Scott Berceli[4,5]

[1] Houston Methodist Research Institute, Houston, TX, USA
[2] Department of Surgery, Houston Methodist Hospital, Houston, TX, USA
[3] LaSIE, UMR CNRS 7356, University of La Rochelle, La Rochelle, France
[4] Department of Surgery, University of Florida, Gainesville, FL, USA
[5] Malcom Randall VAMC, Gainesville, FL, USA
garbeymarc@gmail.com

**Abstract.** Failure of peripheral endovascular interventions occurs at the intersection of vascular biology, biomechanics, and clinical decision making. It is our hypothesis that most of the endovascular treatments share the same driving mechanisms during post-surgical follow-up, and accordingly, a deep understanding of them is mandatory in order to improve the current surgical outcome. This work presents a versatile model of vascular adaptation post vein graft bypass intervention to treat arterial occlusions. The goal is to improve the computational models developed so far by effectively modeling the cell-cell and cell-membrane interactions that are recognized to be pivotal elements for the re-organization of the graft's structure. A numerical method is here designed to combine the best features of an Agent-Based Model and a Partial Differential Equations model in order to get as close as possible to the physiological reality while keeping the implementation both simple and general.

**Keywords:** Vascular Adaptation · Particle Model · Immersed Boundary Method · PDE Model

## 1 Introduction and Motivation

The insurgence of an arterial localized occlusion, known as Peripheral Arterial Occlusive Disease (PAOD), is one of the potential causes of tissue necrosis and organ failure and it represents one of the main causes of mortality and morbidity in the Western Society [1, 3].

In order to restore the physiological circulation, the most performed technique consists into bypassing the occlusion with an autologous vein graft. Benefits and limitations of this procedure are driven by fundamental mecano-biology processes that take place immediately after the surgical intervention and that fall under the common field of vascular adaptation.

* NIH UO1 HL119178-01

ICCS Camera Ready Version 2018
To cite this paper please use the final published version:
DOI: 10.1007/978-3-319-93701-4_68

Today the rate of failures of Vein Graft Bypass (VGBs) as treatment for PAODs remains unacceptably high [4], being the graft itself often subjected to the post-surgical re-occlusive phenomenon known as restenosis. It is our belief that the causes of such failures need to be searched for within the multiscale and multifactorial nature of the adaptation that the graft faces in the post-surgical follow-up in response to the environmental conditions variations, a process commonly known as vascular adaptation.

Fig. 1 offers a detailed description of the cited nature of adaptation, where sub-sequent and interconnected variations at genetic, cellular and tissue level concur to create a highly interdependent system driven by several feedback loops.

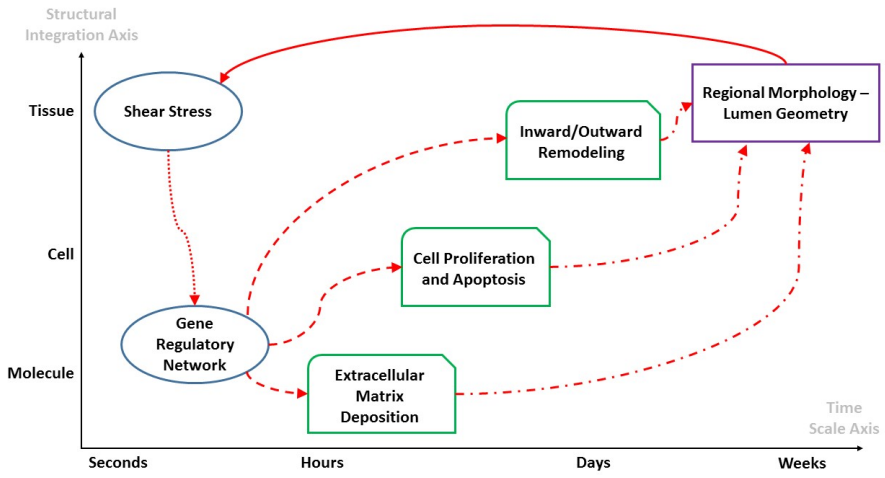


**Fig. 1.** Multiscale description of vascular adaptation: dynamic interplay between physical forces and gene network that regulates early graft remodeling [7].

The goal of this work is to address the modeling and simulation of the vascular adaptation from a multiscale perspective, by providing a virtual experimental framework to be used to test new clinical hypotheses and to better rank the many factors that promote restenosis. In addition, our hypothesis is that an accurate implementation of the potential forces governing cellular motility during wall rearrangement is mandatory to obtain a model close enough to the physiological reality. From a qualitative observation of histological evidences, a sample of which is shown in Fig. 2, local distribution of cells across the wall is relatively uniform and we supported that this feature provides some interesting guidances on what the dominant biological mechanism of cellular motility might be.

This study is based on the extensive work carried out by our group on vascular adaptation [5, 7] and it represents a big step toward a more accurate replication of the physiological reality thanks to its ability of taking in account pivotal bio-

ICCS Camera Ready Version 2018
To cite this paper please use the final published version:
DOI: 10.1007/978-3-319-93701-4_68

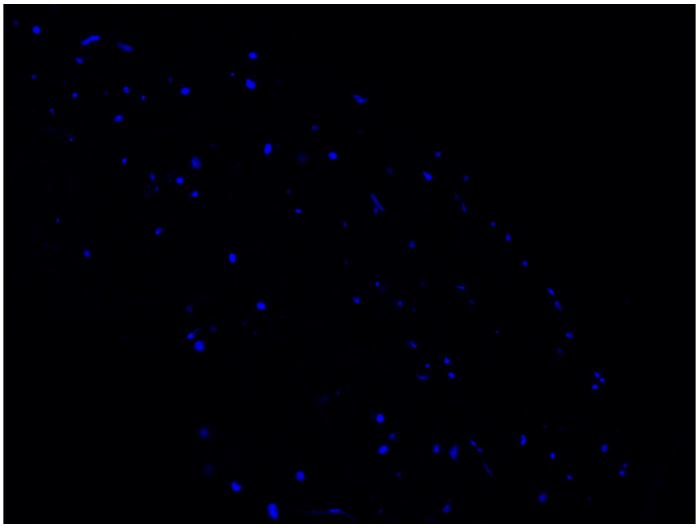

**Fig. 2.** Staining image of a portion of graft's wall: the blue dots identify the cells' nuclei, the stack of images were obtained via confocal microscopy and post-processed in order to correct the artifacts due to the different depths of cells with respect to the plan of visualization.

logical events such as cellular motility and cell-cell, cell-membrane interactions, which in reverse were very difficult to represent with a discrete Agent-Based Model (ABM) implemented on a fixed grid [5]. The adaptation is here replicated on a 2D cross section, a choice justified by the fact that cited data from histology used to qualitatively validate the model are available in the format of a 2D slice. Finally, the model has been cross-validated against a Dynamical System (DS) [11] and the ABM [5] previously cited, a never-trivial feature for a computational model, as it allows to choose the best model to be used according to the purpose of the analysis performed.

## 2 Methods

In order to replicate the anatomy of the graft, the computational model is organized in 4 sub-domains shown in Fig. 3 that are lumen, tunica intima and media, and external surrounding tissue, where intima and media are separated by the Internal Elastic Lamina (IEL).

The numerical model can be decomposed in three sub-sections respectively corresponding to a software module working on different scales - see Table 1:

– **Mechanical Model (MM):** it locally computes the value of mechanical quantities of interest, such as flow velocity, shear stress, strain energy, *et cetera*.

ICCS Camera Ready Version 2018
To cite this paper please use the final published version:
DOI: 10.1007/978-3-319-93701-4_68

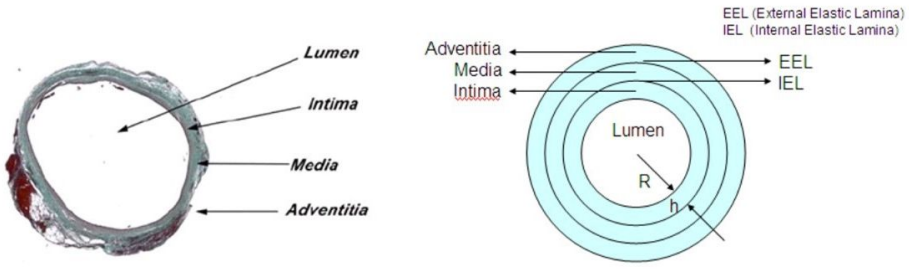


**Fig. 3.** Morphological structure of a vein graft: between the intima and the media is the Internal Elastic Lamina (IEL) and the External Elastic Lamina (EEL) is between the media and the adventitia [2].

- **Tissue Plasticity (TP):** it defines the driving cellular events, mainly cellular mitosis/apoptosis and matrix deposition/degradation, as stochastic laws driven by constant coefficients.
- **Tissue Remodeling (TR):** it computes the re-organization of the graft structure driven by cellular migration.

**Table 1.** *Multiscale nature of the hybrid model*

| space scale versus time scale | second | hour | day |
|---|---|---|---|
| $10^{-4}m$ | | TR | TP |
| $10^{-3}m$ | MM | TR | |
| $10^{-2}m$ | MM | | |

The MM is described by a Partial Differential Equations (PDEs) of continuous mechanics [8], TP with an ABM regulating the cells behavior [6, 5], and TR by particles moving in a highly viscous incompressible media, which cells motion is computed on the base of a continuum space. The most challenging part is the definition of the forces that drive the cellular motility toward the re-organization of the graft in a way both biologically accurate but also mathematically simple in order to be able to easily calibrate the formula on experimental data for validation purposes. As anticipated in the Introduction, the cornerstone of our model is its multiscale nature and so the numerical discretization and the algorithm implemented for each module will encompass multiple scales both in time and in space detailed in Table 1.

ICCS Camera Ready Version 2018
To cite this paper please use the final published version:
DOI: 10.1007/978-3-319-93701-4_68

### 2.1 Mechanical Model (MM)

The blood flow in the lumen is described as a steady incompressible flow that remains constant independently from the inward/outward nature of the remodeling and, accordingly, the standard set of equations of a flow through a pipe was used to simulate such flow across the vein assuming a non-slip condition at the wall [8, 9]. The MM computes the flow and the shear stress at the wall, labeled as $\tau_{wall}$, and both variables are updated at every step if the lumen geometry variation is greater than a certain tolerance, in formula:

$$distance(\partial\Omega^{new}_{lumen}, \partial\Omega^{old}_{lumen}) \; > \; tol,$$

where distance is intended as the Euclidean distance between two consecutive time points on the same lumen location and $tol \approx 10^{-4}m$, i.e. a cell diameter. The deformation of the wall can be described both with a thick cylinder approximation, easily computable with a Matlab code [10], or by a Neo-Hookean hyperelastic model, computable by using a finite element technique with FEBio software [9]. The description of the tissue mechanical properties is the one adopted in previous works by our group [5, 7, 11], and accordingly, being the wall displacement negligible, the strain energy ($\sigma$) becomes the main element influencing cellular metabolism within the media. Finally cellular division is driven by the diffusion of a generic Growth Factor (GF) across the wall, which sees in the shear stress its driving force. Denoting it with $G(\tau)$, the GF diffusion is defined as:

$$\frac{\partial G}{\partial t} = c \; \Delta G \; in \; \Omega, \; G_{|\partial\Omega_{lumen}} = F(\tau_{wall}), \; \frac{\partial G}{\partial n} \; |\partial\Omega = 0, \tag{1}$$

where c is the diffusion coefficient.

### 2.2 Tissue Plasticity (TP)

Cellular and ExtraCellular Matrix (ECM) activity is described with an ABM-based implementation [12], mostly relying on a cellular automata principle governed by stochastic laws, such as each cellular event is associated to a density of probability. We refer to [5, 6] for a detailed description of the algorithm, and for completeness, Table 2 provides an axiomatic description of the rules that drive the ABM.

The stochastic model describes how the cellular events depend on the local concentration of the associated GF (1), triggered by shear stress within intima and strain energy within media, creating in this way the bridge between continuum mechanics and TP. Early restenosis is mostly attributable to Intimal Hyperplasia (IH), i.e. an un-controlled growth of the intima toward the lumen, for which a reduction of shear stress stimulates specific GFs to switch their status from quiescent to active. The latter promotes cellular migration toward the intima with subsequent proliferation and deposition of ECM.

To simulate the switching from a normal condition to a perturbed one, representing the response of the system to an environmental conditions variation, the key is to define a so-called basic solution, where the system is stable and

ICCS Camera Ready Version 2018
To cite this paper please use the final published version:
DOI: 10.1007/978-3-319-93701-4_68

**Table 2.** *Axiomatic Description of the Set of Rules of the ABM*

| Rule | Variable | Function |
|---|---|---|
| $p_{division} = p_{apoptosis} = \alpha_1,$ | SMC | SMC equilbrium in Basic Solution |
| $p_{degradation} = p_{production} = \alpha_2,$ | ECM | ECM balance in Basic Solution |
| $A(t) = \exp -\frac{t-T}{\delta T};\ T = \alpha_3,\ \delta T = \alpha_4$ | all | factor all probability laws by macrophage activity |
| $T$ and $\delta T$ | macrophage | time of maximum macrophage activity and relaxation time |
| $p^I_{division} = \alpha_1 A(t)(1 + \alpha_5 \frac{G(\Delta\tau)}{\bar{\tau}})$ | SMC | probability of SMC division in intima. |
| $p^I_{apoptosis} = \alpha_1 A(t)$ | SMC | probability of SMC apoptosis in intima. |
| $p^I_{production} = \alpha_2 A(t)(1 + \alpha_6 \frac{\Delta\sigma}{\bar{\sigma}})$ | ECM | probability of ECM production in media. |
| $p^I_{degradation} = \alpha_2 A(t)$ | ECM | probability of ECM degradation in media. |
| $p_{migration} = \alpha_7 A(t)(1 + \alpha_8 \frac{G(\Delta\tau)}{\bar{\tau}})$ | SMC | probability of SMC migration from intima to media. |

regulated by standard conditions that ensure a fair balance both for cellular mitosis/apoptosis and for ECM synthesis/degradation. Intuitively, the basic solution represents a healthy vein at time of implant and the perturbed model will evolve driven by mechanical forces in order to recover the perturbation applied and to reach back the equilibrium. To simulate the restenosis process, a perturbation of shear stress will be applied in order to promote IH.

### 2.3 Tissue Remodeling (TR)

The biggest novelty of the model consists into the abandonment of a fixed grid-based structure, used so far [5], in favor of a continuous mechanic description. Accordingly, Smooth Muscular Cells (SMCs) are now described as discs of radius $R_{SMC}$ crawling in a highly viscous flow, and not anymore like dynamic state

ICCS Camera Ready Version 2018
To cite this paper please use the final published version:
DOI: 10.1007/978-3-319-93701-4_68

variables allocated on a static hexagonal grid. As per biological evidences, SMCs can synthetize or degrade ECM, in addition to undergoing mitosis/apoptosis. This generates a source and a sink term respectively in the mass balance that will be used to determine the energy of the structure. The adaptation consists into the response of the structure to an energy unbalance, which sees the reorganization of the system driven by cellular motility in order to recover toward a condition of equilibrium. Remembering that each layer of the graft is bounded by an elastic membrane, the considerations highlighted naturally suggest the use of an Immersed Boundary Method (IBM) [13] in order to simulate the remodeling of the structure, which is so articulated in three phases: i) an IBM algorithm to take in account SMCs activity and membranes adjustment; ii) an SMCs motion algorithm; iii) an inward/outward remodeling algorithm.

**IBM Algorithm** A time-split numerical implementation drives the tissue remodeling, meaning that while the TP model is run with a time step of 1 hour, the IBM algorithm is run with a variable time step $\delta t$ that corresponds to the relaxation time of the media with respect to cell division and motility: the larger $\delta t$ the more cylindrical the graft will end to be. The spatial resolution with step h is linked to the Cartesian nature of the grid and it is chosen to be of the order of a SMC radius. Since the media is described as a highly viscous fluid, we compute the variables V and P, respectively velocity and pressure of the fluid. The IBM algorithm is applied to a square domain $\omega = (0,1)^2 \in \mathbb{R}^2$ in which the vein graft section is embedded. The wall and lumen boundaries of the vein graft and interfaces separating intima from media, see Fig. 3, are described by immersed elastic boundaries: let us denote $\Gamma \in \Omega$ a generic immersed elastic boundary with curvilinear dimension one. $X$ is the Lagrangian position vector of $\Gamma$, expressed in the 2-dimensional Cartesian referential. The Lagrangian vector $f$ is the local elastic force density along $\Gamma$, also expressed in the Cartesian referential. $f$ is projected onto $\Omega$ to get the Eulerian vector field $F$, that corresponds to the fluid force applied by the immersed elastic boundaries.

If $s \in (0,1)^m$ is the curvilinear coordinate of any points along $\Gamma$, and $t \in [0, t_{max}]$ is the time variable, the different mapping can be summarized as it follows:

$$\begin{aligned} V : (x,t) \in \Omega \times [0,t_{max}] &\longrightarrow \mathbb{R}^2 \\ P : (x,t) \in \Omega \times [0,t_{max}] &\longrightarrow \mathbb{R} \\ X : (s,t) \in (0,1)^m \times [0,t_{max}] &\longrightarrow \Omega \\ f : (s,t) \in (0,1)^m \times [0,t_{max}] &\longrightarrow \mathbb{R}^2 \\ F(x,t) \in \Omega \times [0,t_{max}] &\longrightarrow \mathbb{R}^2 \end{aligned}$$

One of the cornerstones of the IBM method is the formulation of the fluid-elasitc interface interaction, which model is unified into a set of coupled Partial Differential Equations (PDEs). To build that, the incompressible Navier-Stokes

ICCS Camera Ready Version 2018
To cite this paper please use the final published version:
DOI: 10.1007/978-3-319-93701-4_68

system writes:

$$\rho\left[\frac{\partial V}{\partial t}+(V.\nabla)V\right]=-\nabla P+\mu\Delta V+F \tag{2}$$

$$\nabla.V=0 \tag{3}$$

The IBM algorithm requires the extrapolation of the Lagrangian vector $f$ into the Eulerian vector field $F$ from the right end side of (2). For this purpose a distribution of Dirac delta functions $\delta$, is used, such as:

$$F(x,t)=\int_{\Gamma} f(s,t)\delta\left(x-X(s,t)\right)ds=\begin{cases}f(s,t), & \text{if } x=X(s,t)\\ 0, & \text{otherwise}\end{cases} \tag{4}$$

Its dynamic is regulated with a linear elastic model implemented by using the Hooke law of elasticity, for which the tension of the IB is linear function of the strain energy. The local elastic force density assumes its final form that writes

$$f(s,t)=\sigma\frac{\partial^2 X(s,t)}{\partial s^2}. \tag{5}$$

The IBM algorithm offers dozens of potential possibilities of implementation: the rationale should always be to pursue the right compromise between stability of the scheme and accuracy. Because the fluid is highly viscous, a standard projection scheme for the Navier Stokes equations discretized with finite differences on a staggered grid was used. The momentum equation was discretized with central second order finite differences for the diffusion term and with a method of characteristic for the convective term.

**SMC motility** The second phase of tissue remodeling consists into the computation of SMCs motility. The algorithm to compute the trajectory can be divided in two consecutive steps.

First, SMCs move passively in the matrix by following the media on the base of the local velocity field with the same numerical scheme applied to the discrete point of the immersed boundary, and second, SMCs move also actively driven by multiple potential driving forces, listed below:

- SMCs interact each others. A description of such interactions based on an analogous of the Lennard-Jones potential looks like a smart choice to define an initial framework. Under this hypothesis, during mitosis the two cells may spearate and remain at a distance of about their diameter. This makes the two Lennard-Jones potential coefficients to be cellular size-dependent.
- Further motion of SMCs depends on the gradient of molecules density that are the solution of a reaction-convection diffusion system. Accordingly a generic GF has been introduced with (1) in order to describe the chemotaxis that is originated by the cited gradient.
- Cell motility has a random component that participates to their diffusion through the tissue.

ICCS Camera Ready Version 2018
To cite this paper please use the final published version:
DOI: 10.1007/978-3-319-93701-4_68

– SMCs may infiltrate area free of cells to preserve the tissue integrity. This motion corresponds to a mechanical homeostasis and it maintains a local balance between SMC and ECM distribution to keep the matrix healthy [14, 15].

The trajectory of a SMC can be so described by tracking its position along time with the following relation:

$$\dot{X} = V_S + V_E + V_G + V_R, \tag{6}$$

where $X$ is the location of the single SMC.

In (6), $V_S$ sums up the repulsive forces between particles. The amplitude of this force decays with the distance and, in first approximation, one can assume a linear decay toward zero in $n_S$ units expressed in cell diameter. Consequently, cell-cell interaction is only possible between elements belonging to the same subdomain, i.e. intima or media, and also interaction is not possible between cells separated by a distance larger than $2\ n_s\ R_{SMC}$, where $n_s$ has been chosen to be of the order of few units.

$V_E$ sums up the attractive forces between the particles that decay linearly as for the cell interaction but in $n_e$ units and become zero above a distance of $2\ n_e\ R_{SMC}$. $n_s$ and $n_e$ have a great influence on the result of the simulation and a deep analysis of them will be useful to address some open problems of the vein graft's biology.

$V_G$ is proportional to the gradient of $G$ that is the generic GF that activates SMC proliferation.

Finally, $V_R$ is a random vector that mimics the noisy character of cell motility. Its intoduction is justified by the assumption that a cell can not move more than a radial unit within the time step $\delta t$ of the IBM algorithm.

The strong feature of the method here proposed is that it allows us to implement all these elements that are known to play a key role at biological level and to also test several combinations of them. However, compared to our previous ABM [5], the number of unknown parameters used to describe the new cellular motility module grows proportionally with the level of closeness of the model to the physiological reality, and accordingly, a non-linear stability analysis will be needed to find the trade-off between complexity and accuracy as already done in [6].

**Inward Outward Membrane Motion Adjustment** An *ad hoc* adjustment is needed in order to prevent the structure to always promote outward remodeling, seen the incompressibility of the lumen medium. The hypothesis is so that the tissue accommodates to the transmural pressure that is a combination of blood pressure and external pressure from the surrounding tissue toward a state that gives less mechanical stress on cells. This adjustment is still driven by an energy minimization logic, for which at each cycle, the mechanical energy of the wall is computed with the MM and the sign of a sink/source term is decided in accordance with the sign of the derivative that minimizes said energy. Finally,

ICCS Camera Ready Version 2018
To cite this paper please use the final published version:
DOI: 10.1007/978-3-319-93701-4_68

in order to improve the model, we need to consider i) that macrophages in the wall can be treated with the same framework but of course by adjusting the related parameters; ii) that the IEL has a certain porosity allowing SMCs to pass through and iii) that the volume of a daughter cell can increase in time.

## 3 Plan of Simulations

As previously mentioned, a basic solution needs to be retrieved in order to serve as baseline point for the vascular adaptation simulation. The setup to retrieve it and the rationale for the representation of the results are the same already used in [6], and the same is valid for IH, which was then simulated by studying both its early phase (1 day follow up) and its late phase (1 month). After all, a comparison between the two phases is important in order to distinguish the different impact of the several aims of SMCs motility.

Finally, a cross validation between the presented model and a DS developed by our group [11] has been performed on a 4 months follow-up as also done for the original ABM [5] with the motivations highlighted in the Introduction.

In order to perform the cross validation, the DS has been setup with a 50% decrease in shear stress from the baseline value to foster the hyperplasia with initial graft (R), lumen (r), and IEL (re) respectively equal to R = 0.2915, re = 0.2810, and r = 0.2387, all expressed in mm. It is finally important to recall how, in order to calibrate the DS on the new PDE model, the distance between the two models output, temporal intimal area dynamic in this case, has been minimized by using a Genetic Algorithm (GA).

## 4 Results

Fig. 4(a) shows the generation of the basic solution. Each red dot corresponds to a SMC, while the green circle individuates the IEL. It is important to recall how our modeling effort has been driven by the pursuit of a graft's cross section that shows a uniform distribution of cells across the wall also free from isolated cells occurrence. Already the replication of the initial condition represents a good approximation of the grafts histology. The analysis of the early stage of hyperplasia offers a nice overview of how the accuracy of the model grows along with the number of forces driving SMCs motion implemented. Here SMCs in intima and media are respectively individuated by a red and a black circle, while the IEL lamina is still shown in light green.

Fig. 4(b) reports a first example of early stage of IH, where the random motion is the only component driving the adaptation of the strucures. As it is clear from the figure, a uniform distribution of SMCs is not reached in the intima as instead retrievable from a comparison with histology and this is mainly caused by the motion restriction that affects SMCs because of the reduced initial thickness of the intima. By adding the repulsive cell-cell interaction, the distribution of SMCs gets more uniform, as appreciable in Fig. 4(c), even though the formation of clusters that will eventually be trapped in pockets of the lumen wall and

ICCS Camera Ready Version 2018
To cite this paper please use the final published version:
DOI: 10.1007/978-3-319-93701-4_68

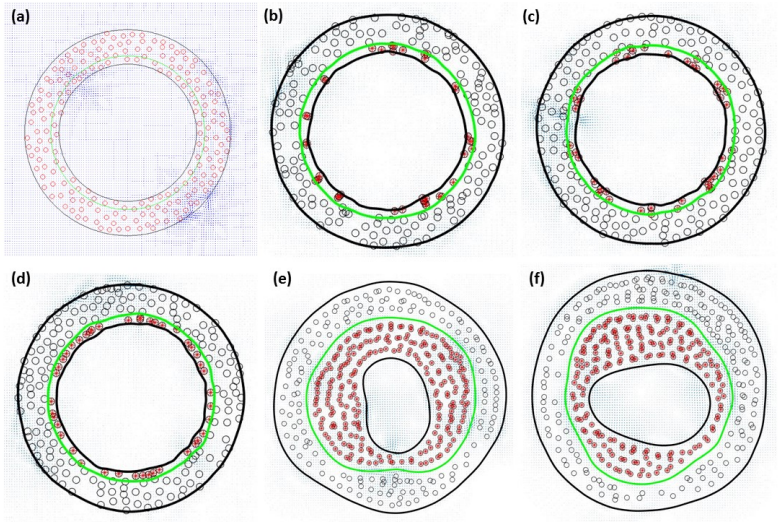


**Fig. 4.** Cross Section of the vein graft reported in (a) basic solution, i.e. healthy vein condition; early stage of hyperplasia progressively adding up (b) random motion, (c) cell-cell repulsion, and (d) matrix invasion forces; late phase of hyperplasia encroaching the lumen affected by (e) vertical and (f) horizontal stretching of the lumen itself.

there confined by the membranes tension is still clearly visible. Also important to point out is the tendency that some areas of ECM with no SMCs have to form, taking in this way the model far from the reality observed at histology level.

A more uniform distribution is reached by adding the matrix invasion term as shown in Fig. 4(d), corroborating in this way the belief that an accurate description of SMCs motion is the key in order to obtain a model close enough to the physiological reality. As side consideration, accordingly to the purpose of this work, SMCs proliferation within the media has not been activated, and so it was to be expected a regular uniform distribution of cell within the media layer.

Fig. 4(e) and Fig. 4(f) report the result of two independent simulations run with a follow-up of 4 months in order to study the late phase of IH. It is interesting to see how the SMCs distribution retains its asymmetric character, either in a vertical or in a horizontal direction, even though it is not clear if this is justified at histological level or not. If necessary, to promote radial symmetry, a potential solution will be to suppose that SMCs motility has a preferred motion in the direction orthogonal to the radius in order to align the cell arrangement with the dominant radial strain energy. Coupled to it, an increase in the relaxation time t might be another way to further incentivize SMCs distribution toward radial direction.

Finally, in order to cross-validate the DS and the PDE model, the first step was to reproduce the qualitative patterns of IH with this latter, the results of which can be appreciated in Fig. 5, where the temporal dynamic of lumen area

ICCS Camera Ready Version 2018
To cite this paper please use the final published version:
DOI: 10.1007/978-3-319-93701-4_68

(a), intimal area (b), and medial area (c) are represented. It is useful to remark how, in every panel, each independent simulation is marked with a different color and the average trend, in bold black line, serves as representative one. Finally, the result of the calibration, taking as output the temporal dynamic of lumen area, is reported in Fig. 5(d), showing a high level of accuracy with a percentile error lower than 2%.

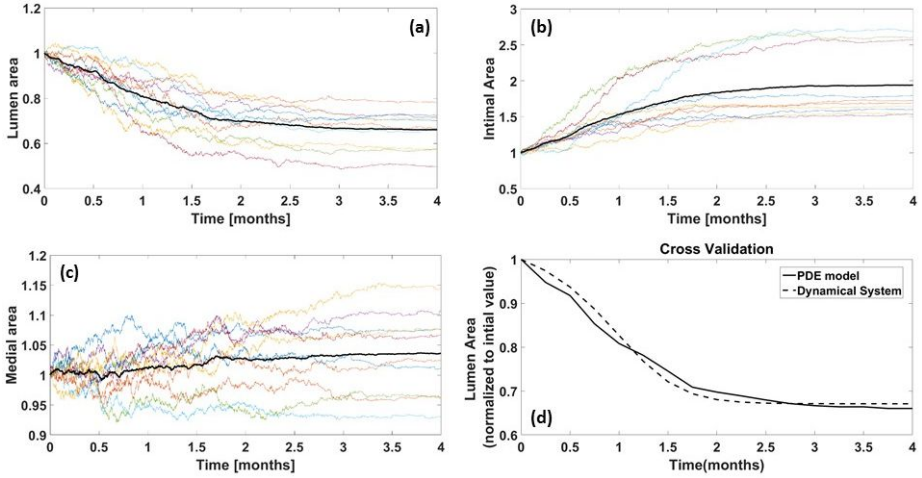


**Fig. 5.** Intimal Hyperplasia long term follow-up: temporal dynamic of (a) lumen area, (b) intimal area, and (c) medial area are represented on a 4 months follow-up. Each plot is normalized on the initial value and the output evaluated by taking the average trend (black bold line) out of 10 independent simulation (color lines). Finally, as cross validation in (d), the Dynamical System is calibrated on the mean output of the PDE model (solid line) against the mean output of the DS (dashed line).

## 5 Conclusion

In the current work, a model of vascular adaptation has been implemented as a generalization of a previous ABM developed by our group. With the new approach we abated the limitation imposed by the use of a fixed grid by using a technique that relies almost entirely on PDEs and differential equation to compute the plasticity of the wall and the motility of the cells. As appreciated in the Results section, the key point to obtain an accurate model consists into the right definition of the forces that drive SMCs motion and of course in their effective implementation. After all, one of the power of the model is exactly its ability to test different hypothesis at computational level in a short time and in an effective way. Two evidences can be learn from our model. First, to consider the invasion of the matrix operated by SMCs is pivotal to maintain

ICCS Camera Ready Version 2018
To cite this paper please use the final published version:
DOI: 10.1007/978-3-319-93701-4_68

mechanical homeostasis [15] and consequently to reproduce experimental data accurately. Second, the definition of the distance threshold that operates the different cell-cell interaction forces are as much important. The obvious next step is the extension of the model toward the third dimension along with an extensive study of data from histology in order to better reconstruct the initial structure of the vein. Finally, the recent work published by Browning et al. [16], based on prostate cancer cell lines, gives an excellent example of what should come next in this vascular adaptation study. Further validation of the model with quantitative metrics on density map of cell migration an spatially accurate proliferation and apoptosis rate is underway and will require extensive post-processing of our experimental data set.

## References


1. Go AS, et al.: American Heart Association Statistics Committee and Stroke Statistics Subcommittee. Heart disease and stroke statistics2014 update: A report from the American Heart Association. Circulation **129**(3), e28-e292 (2014)
2. Jiang Z, et al.: Vein graft model: adaptation to differential flow environments. American Journal of Physiology - Heart and Circulatory Physiology **286**(1), H240-H245 (2004)
3. Roger VL, et al.: Heart Disease and Stroke Statistics - 2012 Update: A Report from the American Heart Association. Circulation **125**(1), e2-e220 (2012)
4. Harskamp RE, et al.: Saphenous vein graft failure and clinical outcomes: Toward a surro-gate end point in patients following coronary artery bypass surgery. Am Heart J. **165**, 639-43 (2013)
5. Garbey M, et al.: Vascular Adaptation: Pattern Formation and Cross Validation between an Agent Based Model and a Dynamical System. Journal of Theoretical Biology **429**, 149-63 (2017)
6. Garbey M, et al.: A Multiscale Computational Framework to Understand Vascular Adaptation. Journal of Computational Science **8**, 32-47 (2015)
7. Casarin S, et al.: Linking gene dynamics to vascular hyperplasia toward a predictive model of vein graft adaptation. PLoS ONE **12**(11), e0187606 (2017)
8. White FT: Viscous Fluid Flow. 2nd edn. McGraw-Hill Series in Mechanical Engineering (1991)
9. Maas SA, et al.: Febio: finite elements for biomechanics. J. Biomech. Eng. **134**(1), 011005 (2012)
10. Zhao W, et al.: On Thick-Walled Cylinder Under Internal Pressure. Journal of Pressure Vessel Technology **125**, 267-73 (2003)
11. Garbey M, et al.: A Multiscale, Dynamical System that Describes Vein Graft Adaptation and Failure. Journal of Theoretical Biology **335**, 209-20 (2013)
12. Deutsch A, et al. Cellular Automaton Modeling of biological Pattern Formation. Birkhuser, Boston (2005)
13. Peskin CS. The immersed boundary method. Acta Numerica **11**, 479-517 (2002)
14. Quaranta V. Cell migration through extracellular matrix: membrane-type metalloprotein-ases make the way. J. Cell. Biol. **149**, 1167760 (2000)
15. Humphrey JD, et al.: Mechanotransduction and extracellular matrix homeostasis. Nat. Rev. Mol. Cell. Biol **15**(12), 802-812 (2014)


ICCS Camera Ready Version 2018
To cite this paper please use the final published version:
DOI: 10.1007/978-3-319-93701-4_68

16. Browning AP, et al.: Inferring parameters for a lattice-free model of cell migration and proliferation using experimental data. Journal of Theoretical Biology **437**, 251-60 (2018)

ICCS Camera Ready Version 2018
To cite this paper please use the final published version:
DOI: 10.1007/978-3-319-93701-4_68